

Static and Time-Dependent CI in Continuum for Multi-Nucleon Transfer Reactions

Aurel Bulgac, University of Washington, Seattle, WA, USA

in collaboration with

Matthew Kafker, University of Washington, Seattle, WA, USA
Cyclotron Laboratory, Texas A&M University, College Station, TX, USA

Based on: A. Bulgac, arXiv:2024.092173, Phys. Rev. C, in press (2026)
M. Kafker and A. Bulgac, arXiv:2604.218454

I will explain what and how it was done.

But not so much why.

Only 16 slides and 5 figures in total.

I will provide the minimum necessary number of equations needed to understand the problem we solved.

We solved numerically all equations on Frontier supercomputer, OCLF.

We needed 80 TB of memory.

We used 48,000 GPUs for the static problem and 56,000 GPUs for the time-dependent problem.

Ours is arguably the largest GCM problem ever simulated.

One can make a parallel between:

the state of technology in the human society

and

the state of quantum description of strongly interacting many fermion systems.

Roughly before 1800 people built roads, bridges, pyramids, castles with one or more floors - in a word static structures - and for transportation used animals and wind.

After 1800 people started building machines and most things were in motion: trains and railways, cars, airplanes, rockets, people landed on the Moon and soon will likely be landing on Mars ...

In quantum mechanics of many-body systems today people construct mostly the equivalent of buildings with one or more floors, and at best the equivalent of skyscrapers with a few hundreds of floors.

Theorists basically do not yet have at their disposal a sufficiently sophisticated quantum time-dependent technology needed for studying the quantum dynamics of non-equilibrium and dissipative phenomena, where interference and entanglement play a dominant role in the dynamics. On the other hand, there are a plethora of phenomenological models, mostly classical in character, with lots of phenomenological parameters and, some would argue, reasonable assumptions.

As an exercise, compare how many time-dependent problems you solved in high and undergraduate schools and how many time-dependent problems you are solving today in quantum mechanics of many-body systems, or even a few bodies.

Quantum mechanics is already more than a century old!

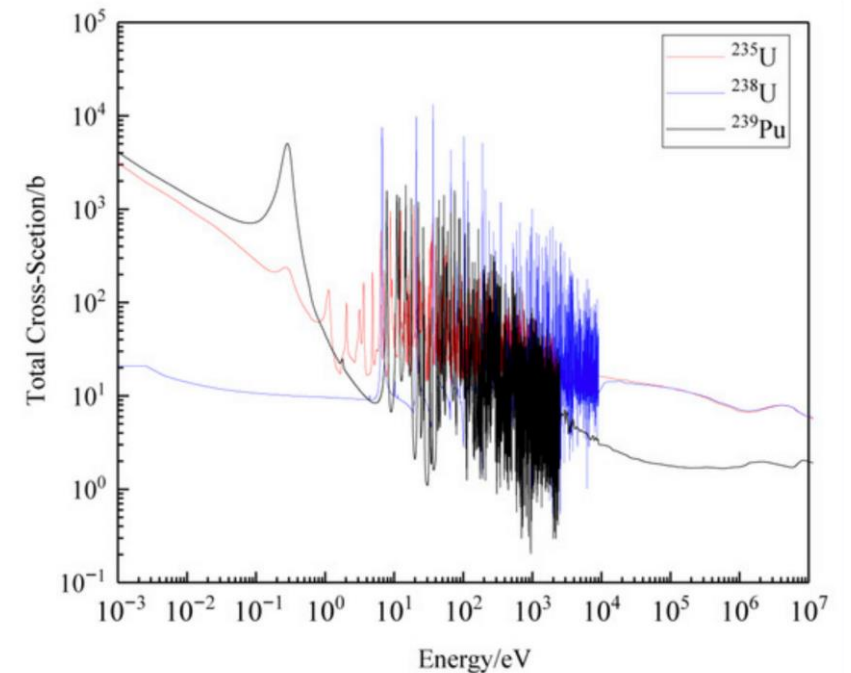
I think, it is correct to say that the great majority of all the known 3,300 isotopes known so far were created in Multi-Nucleon Transfer (MNT) reactions between two colliding nuclei in laboratories worldwide.

We expect that the rest of the unknown 3,500-4,000 isotopes expected to exist and be created in the labs will be created in more or less the same manner.

The MNT reactions are described with the following phenomenological formula for the cross section:

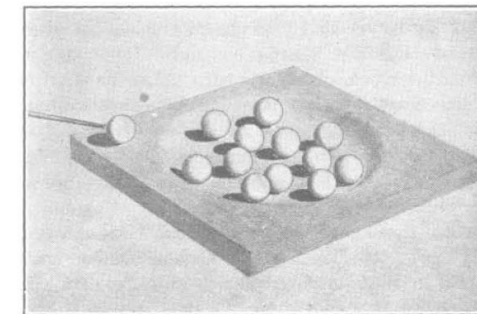
$$\sigma_{EVR} = \sum_{J=0}^{J_{\max}} \sigma_{\text{cap}}(E_{\text{CoM}}, J) P_{\text{CN}}(E^*, J) W_{\text{sur}}(E^*, J)$$

- The first factor in the sum is the capture cross section, which arguably can be evaluated with reasonable accuracy using optical potentials, which typically are phenomenological and for spherical nuclei.
- The second factor is the probability of the formation of the Compound Nucleus (CN), which was never formally derived from a (time-dependent) Schrödinger equation for many nucleons in some form or another.
- The compound nucleus was predicted in 1936 by Niels Bohr (but never derived) and experimental results (crystal blocking) apparently appear to agree with its presence in nuclear reactions and supporting its long life-time.
- The third factor is the probability of “evaporation” of the reaction products, for which there are apparently reasonably trustworthy (semi-)microscopic models: Weiskopf (1937), Hauser and Feshbach (1952) and Ericson (1960).



Experimental total neutron cross-section for three nuclei.

CN appears at incident neutron energies > 10 eV!



This figure never appeared in Bohr's 1936 paper.

What are the essential ingredients of a microscopic theory for strongly time evolving interacting many-body systems?

The equations should:

- Describe phenomena in terms of many-body wave functions,
 - Various components add up with complex time-dependent coefficients, thus capable of describing time evolution,
 - The explicit presence of the Planck's constant.
-
- The dynamics should describe:
 - Interference,
 - Entanglement,
 - The increasing complexity in time of the many-body wave function, the increasing entropy for an isolated system,
 - Dissipation, non-equilibrium quantum dynamics,
 - Thermalization of an isolated quantum system (is the Eigenvalue Thermalization Hypothesis really valid?).

The static CI solution in the continuum for the reaction $^{48}\text{Ca}+^{208}\text{Pb}$.

This is a typical combination of reaction partners in creating transuranium elements.

There will be 3 figures for the static part.

- I will present results for the collision $^{48}\text{Ca}+^{208}\text{Pb}$ in a simulation cubic box $(64 \text{ fm})^3$, with a lattice constant 1 fm.
 - 235 MeV kinetic energy in the center of mass reference system, just above the Coulomb barrier.
- We solve TDHF equations for 152 impact parameters in the orange ring in the plane of the impact parameters.

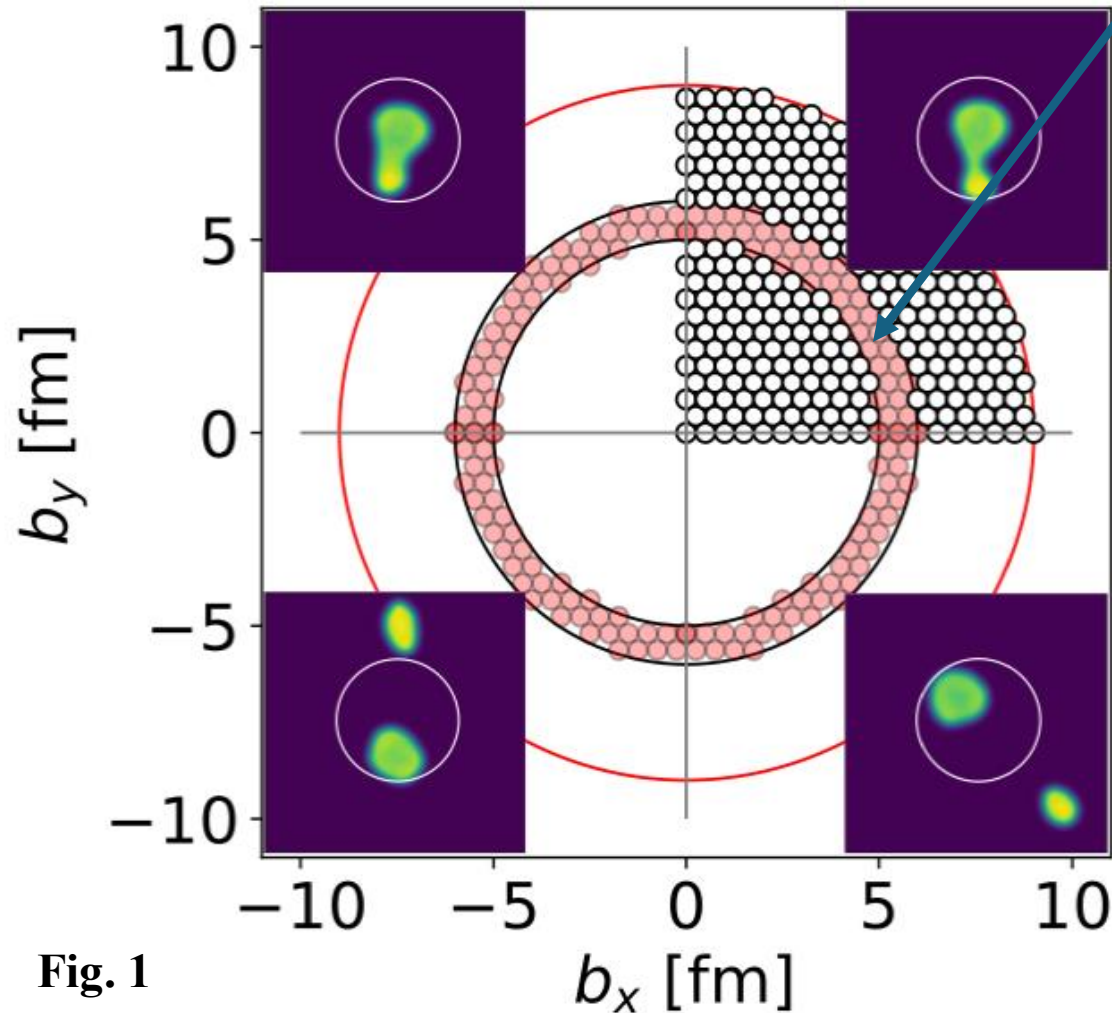


Fig. 1

Impact parameters considered $5 \leq b \leq 6$ fm.

- In the left images TDHF trajectories with $b = 5$ fm.
- In the right images TDHF trajectories with $b = 6$ fm.
- At the top, the two reaction partners come into contact.
- At the bottom, the two reaction fragments are spatially separated

Let me proceed with outlining our approach.

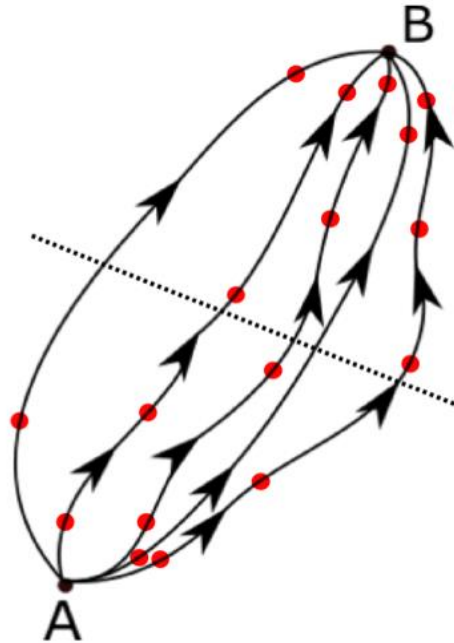


FIG. 2. These are five of the infinitely many paths available in case of neutron induced fission from point A (the time of impinging neutron impact) to point B (detector) at a later time. This figure with added interaction times at random positions (red dots) is reproduced from Wikipedia entry *Path integral formulation*, is a pictorial representation of a many-body quantum propagator $K(\xi_1 \dots \xi_A, \tau | \xi'_1 \dots \xi'_A, \tau')$ from point A at time τ' to point B at time τ .

- Each of these oriented lines are the equivalent of TDHF trajectories in MNT reactions or in induced fission, which are stored in time at the position of the red dots.
- At each time during the evolution the true many-body wave function of the many-body system is a quantum superposition of many time-dependent Hartree-Fock (TDHF) trajectories.
- The final many-body wave function is a coherent superposition of all red dots (TDHF) above the dotted line.
- This last statement might appear incorrect. I will show that it is correct.

- For each impact parameter we follow in time the two reaction partners in TDHF,
- We store the full Slater determinants for the system $^{48}\text{Ca} + ^{208}\text{Pb}$ with a time step $\Delta\tau = 6.4 \text{ fm}/c$, in total approximately 385 instances in time for each impact parameter (more for $b = 5 \text{ fm}$ and less for $b = 6 \text{ fm}$),
- In total we end up with non-orthogonal 39,630 Slater determinants, each denoted by $\Phi(\alpha)$, where $\alpha = (b_x, b_y, \tau)$, but linearly independent Slater determinants for all 256 nucleons.

$$\int_{\alpha'} \langle \Phi(\alpha) | \Phi(\alpha') \rangle g_k(\alpha') = \nu_k g_k(\alpha), \quad \nu_k > 0.00112,$$

$$\int_{\alpha} g_k^*(\alpha) g_l(\alpha) = \delta_{kl}, \quad \int_{\alpha} g_k(\alpha) g_k^*(\beta) = \delta(\alpha - \beta),$$

$$|\bar{\Phi}_k\rangle = \int_{\alpha} \nu_k^{-1/2} g_k(\alpha) |\Phi(\alpha)\rangle, \quad \nu_k > 0, \quad \langle \bar{\Phi}_n | \bar{\Phi}_m \rangle = \delta_{nm}$$

$$\langle \bar{\Phi}_k | \hat{H} | \Psi_n \rangle = \int_l \langle \bar{\Phi}_k | \hat{H} | \bar{\Phi}_l \rangle h_{ln} = h_{kn} E_n,$$

$$|\bar{\Phi}(\alpha)\rangle = \int_l g_l^*(\alpha) |\bar{\Phi}_l\rangle, \quad \langle \bar{\Phi}(\alpha) | \bar{\Phi}(\beta) \rangle = \delta_{\alpha\beta},$$

$$\langle \bar{\Phi}(\alpha) | \hat{H} | \Psi_n \rangle = \int_{\beta} \langle \bar{\Phi}(\alpha) | \hat{H} | \bar{\Phi}(\beta) \rangle h_{\beta n} = h_{\alpha n} E_n.$$

$|\bar{\Phi}_k\rangle$ and $|\bar{\Phi}(\alpha)\rangle$

They are orthogonal to each other and the equivalent of Bloch (running waves) and Wannier (localized states) in crystals. These are linear combinations of 39,630 Slater determinants.

The E_n energy spectrum is consistent with a Gaussian Orthogonal Ensemble spectrum.

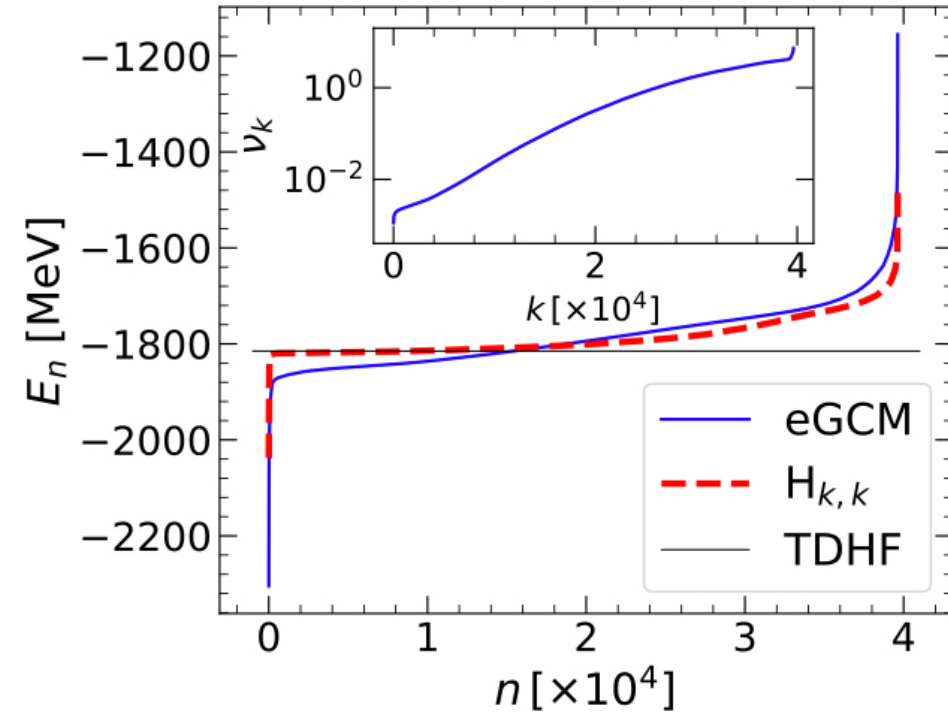


Fig. 2

Inverse participation ratios quantify the delocalization magnitude of a many-body wave function, or the number of major components of a many-body wave function

$$|\bar{\Phi}_k\rangle \quad \text{and} \quad |\bar{\Phi}(\alpha)\rangle$$

$$\text{IPR}_N(k) = \left[\int_{\alpha} |g_k(\alpha)|^4 \right]^{-1}, \quad \text{IPR}_N(\alpha) = \left[\int_k |g_k(\alpha)|^4 \right]^{-1},$$

$$\text{IPR}_H(n) = \left[\int_k |h_{k,n}|^4 \right]^{-1}, \quad \text{IPR}_H(\alpha) = \left[\int_k |h_{\alpha,n}|^4 \right]^{-1}.$$

$$\int_{\alpha'} \langle \Phi(\alpha) | \Phi(\alpha') \rangle g_k(\alpha') = \nu_k g_k(\alpha), \quad \nu_k > 0.00112,$$

$$\int_{\alpha} g_k^*(\alpha) g_l(\alpha) = \delta_{kl}, \quad \int_k g_k(\alpha) g_k^*(\beta) = \delta(\alpha - \beta),$$

$$|\bar{\Phi}_k\rangle = \int_{\alpha} \nu_k^{-1/2} g_k(\alpha) |\Phi(\alpha)\rangle, \quad \nu_k > 0, \quad \langle \bar{\Phi}_n | \bar{\Phi}_m \rangle = \delta_{nm}$$

$$\langle \bar{\Phi}_k | \hat{H} | \Psi_n \rangle = \int_l \langle \bar{\Phi}_k | \hat{H} | \bar{\Phi}_l \rangle h_{ln} = h_{kn} E_n,$$

$$|\bar{\Phi}(\alpha)\rangle = \int_l g_l^*(\alpha) |\bar{\Phi}_l\rangle, \quad \langle \bar{\Phi}(\alpha) | \bar{\Phi}(\beta) \rangle = \delta_{\alpha\beta},$$

$$\langle \bar{\Phi}(\alpha) | \hat{H} | \Psi_n \rangle = \int_{\beta} \langle \bar{\Phi}(\alpha) | \hat{H} | \bar{\Phi}(\beta) \rangle h_{\beta n} = h_{\alpha n} E_n.$$

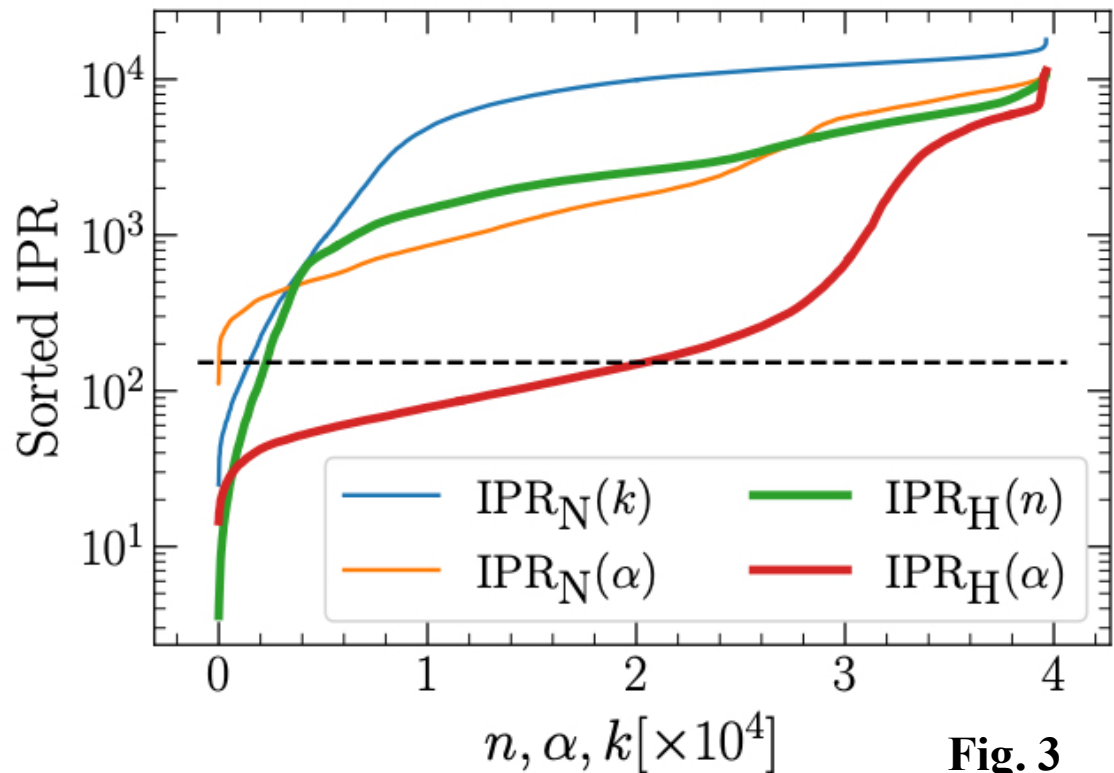
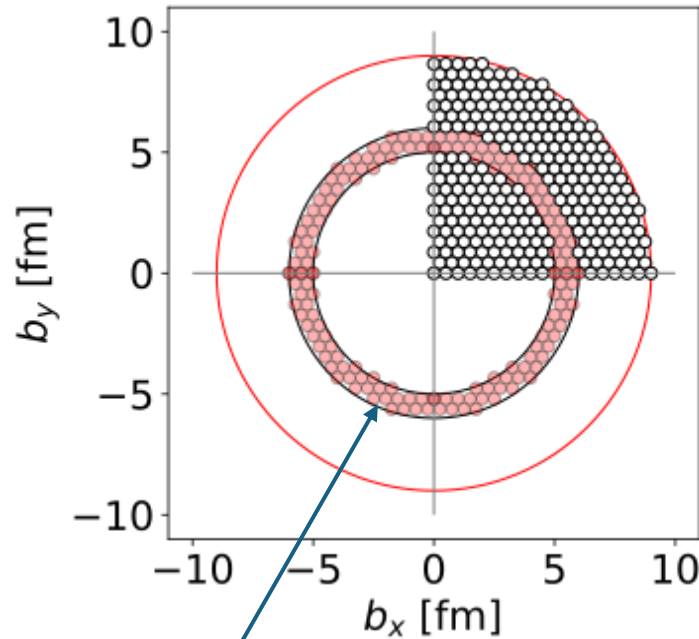


Fig. 3

The time-dependent CI solution in the continuum for the reaction $^{48}\text{Ca} + ^{208}\text{Pb}$, two figures.



$$i\hbar\partial_t|\Psi(t)\rangle = \hat{H}|\Psi(t)\rangle, \quad \langle\Psi(t)|\Psi(t)\rangle = 1,$$

$$|\Psi(t)\rangle = \int_n c_n(t)|\Psi_n\rangle, \quad c_n(t) = c_n(0) \exp\left(-\frac{iE_n t}{\hbar}\right),$$

$$c_n(0) = \langle\Psi_n|\Psi(0)\rangle = \mathcal{N} \int_{\mathbf{b}} \int_{\mathbf{k}} g_k^*(\mathbf{b}, 0) \nu_k^{1/2} h_{kn}^*,$$

Initial many-body state is a superposition of all impact parameters for $^{48}\text{Ca}+^{208}\text{Pb}$ in the ring and moving towards each other in the center of mass system.

$$|\Psi(t)\rangle = \int_k a_k(t)|\bar{\Phi}_k\rangle = \int_{\alpha} d(\alpha|t)|\bar{\Phi}(\alpha)\rangle,$$

“Bloch waves”

“Wannier states”

NB Three different representations of the total time-dependent many-body wave function.

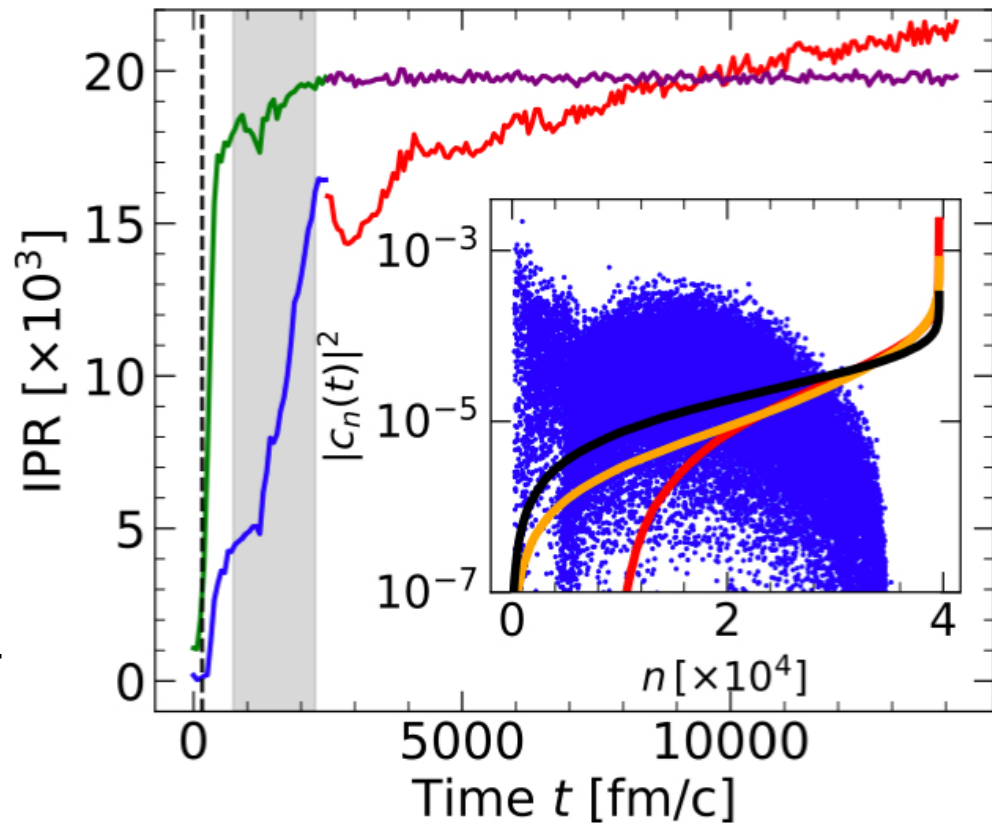


Fig. 4

FIG. 4. The IPR is evaluated for the wave function $|\Psi(t)\rangle$, see Eq. (14), using either the expansion coefficients $a_k(t)$ (blue line, continued red after $t_{fin} = 2,482$ fm/c), and coefficients $d(\alpha|t)$ (green line, continued purple after t_{fin}). The vertical black dashed line indicates the time when all the nuclei first make contact in TDHF. The gray banded region indicates the range of times during which the nuclei separate in TDHF. The inset displays the coefficients $|c_n(t)|^2$, as well as the sorted coefficients $|d(\alpha|t_{fin})|^2$, $|a_k(t_{fin})|^2 \times 1.75$, and $|c_n(t_{fin})|^2$ with black, orange, and red lines respectively.

$$i\hbar\partial_t|\Psi(t)\rangle = \hat{H}|\Psi(t)\rangle, \quad \langle\Psi(t)|\Psi(t)\rangle = 1,$$

$$|\Psi(t)\rangle = \int_n c_n(t)|\Psi_n\rangle, \quad c_n(t) = c_n(0) \exp\left(-\frac{iE_n t}{\hbar}\right),$$

$$c_n(0) = \langle\Psi_n|\Psi(0)\rangle = \mathcal{N} \int_b \int_k g_k^*(\mathbf{b}, 0) \nu_k^{1/2} h_{kn}^*,$$

$$\int_{\alpha'} \langle\Phi(\alpha)|\Phi(\alpha')\rangle g_k(\alpha') = \nu_k g_k(\alpha), \quad \nu_k > 0.00112,$$

$$\int_{\alpha} g_k^*(\alpha) g_l(\alpha) = \delta_{kl}, \quad \int_k g_k(\alpha) g_k^*(\beta) = \delta(\alpha - \beta),$$

$$|\bar{\Phi}_k\rangle = \int_{\alpha} \nu_k^{-1/2} g_k(\alpha) |\Phi(\alpha)\rangle, \quad \nu_k > 0, \quad \langle\bar{\Phi}_n|\bar{\Phi}_m\rangle = \delta_{nm}$$

$$\langle\bar{\Phi}_k|\hat{H}|\Psi_n\rangle = \int_l \langle\bar{\Phi}_k|\hat{H}|\bar{\Phi}_l\rangle h_{ln} = h_{kn} E_n,$$

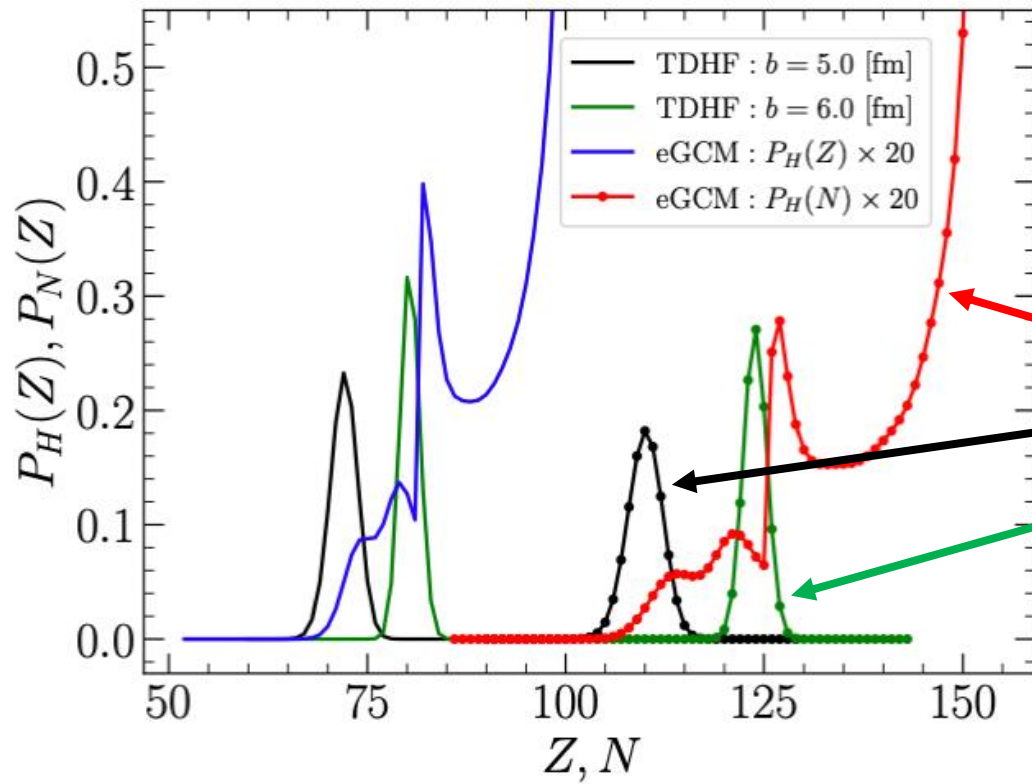
$$|\bar{\Phi}(\alpha)\rangle = \int_l g_l^*(\alpha) |\bar{\Phi}_l\rangle, \quad \langle\bar{\Phi}(\alpha)|\bar{\Phi}(\beta)\rangle = \delta_{\alpha\beta},$$

$$\langle\bar{\Phi}(\alpha)|\hat{H}|\Psi_n\rangle = \int_{\beta} \langle\bar{\Phi}(\alpha)|\hat{H}|\bar{\Phi}(\beta)\rangle h_{\beta n} = h_{\alpha n} E_n.,$$

BTW ETH would predict in this case $\frac{\hbar}{\Delta E} \approx 7 \frac{fm}{c}$.

The “thermalization” appears to be significantly slower, similar to a result we obtained for the UFG Phys. Rev. Res. Letter, 6, L042003 (2024).

Fig. 5



“Newton’s” prediction

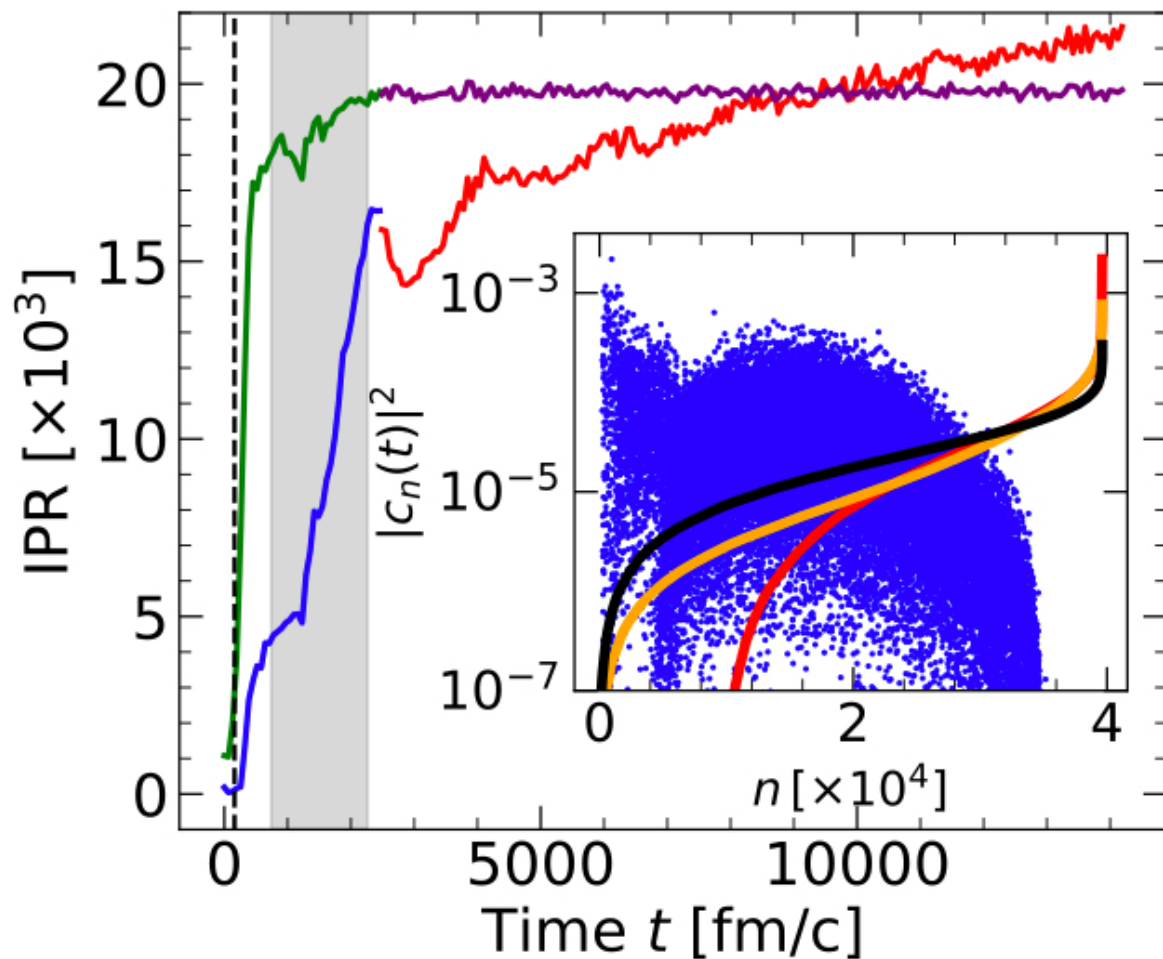
“Young’s” prediction

Notice the factor of 20 needed to make visible the two little bumps!

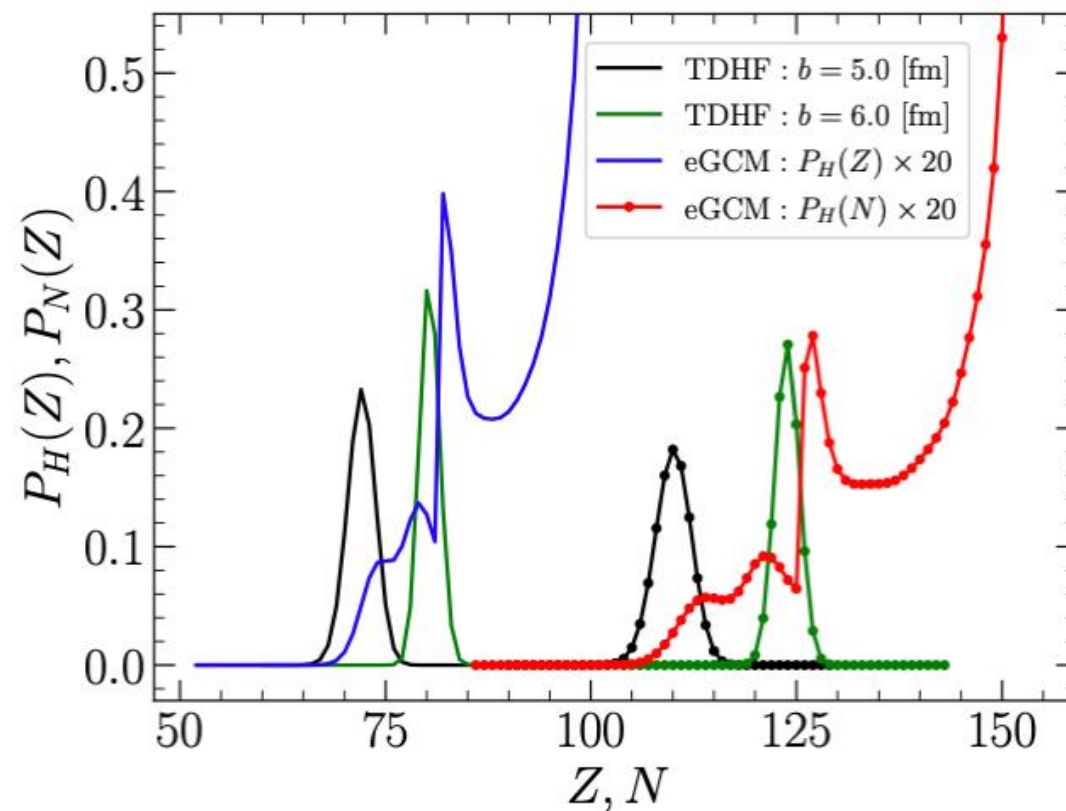
FIG. 5. Final probabilities $P_H(N) = \sum_Z P_H(N, Z)$ (red lines) and $P_H(Z) = \sum_N P_H(N, Z)$ (blue lines) showcasing the dramatic differences between TDHF and eGCM. The solid dotted black and green lines are the TDHF probabilities $P_H(N)$ or $P_H(Z)$ for the heavy fragments and solid without dots for $P_L(N)$ or $P_L(Z)$. The difference between the TDHF and eGCM particle probabilities are as stark as Isaac Newton’s and Thomas Young’s predictions would be for the two-slit experiment.

Apology!

The labels on the ordinate are wrong, but are correctly described in the caption.



Notice how fast the complexity of the many-body wave function evolved from about 100 components to about 20,000 components in a relatively short time. A nucleon at the Fermi level in ^{208}Pb needs approximately 150 fm/c, and longer in the compound nucleus, to go from one end to the other end and back of the nucleus.



Basically in 10-12 nucleon periods the complexity of the many-body wave function increased by a factor of about 150 - 200!

Our CI simulation is what was introduced almost two years ago as the enhanced GCM (eGCM).

Our static and time-dependent CI simulations are de facto the largest type ever of static and time-dependent GCM calculations.

- There is a striking qualitative difference between the TDHF and CI time-dependence, as in Newton vs Young. The images are TDHF!
- In TDHF the two reaction partners are separated at the end of the simulation with probability 1.
- In the TDCI simulation (which emerged in eGCM framework) the **formed compound nucleus** refused to leave the interaction region and the probability to form a heavy system with more protons and neutrons than Pb_{208} is $\sum_{Z=83}^{102} \sum_{N=127}^{154} P(Z, N) = \mathbf{0.85}$. The probability that a system with all nucleons ${}_{102}\text{N}$ is formed and stable during our entire simulation is **0.34**.
- This is (as far as we are aware of) the first microscopic simulation of the formation and evolution of a compound nucleus, conjectured 90 years ago by Niels Bohr (1936).
- These results are an example of the most coherent structures ever shown to exist in nuclear systems. The time-dependent many-body wave function we constructed has about 20,000 components of similar magnitude, evolving from an initial state with only 152 components. Perhaps the most coherent phenomenon identified in nuclear theory is the case of pairing correlations in ${}^{120}\text{Sn}$ (the cleanest condensate in nuclei) where only about 10 Cooper pairs/components (20 neutrons) form a condensate.
- The eGCM many-body wave functions are as important for the nuclear quantum evolution as the Cooper's pair wave function was for superconductivity.

